A nanoelectromechanical systems actuator driven and controlled by Q-factor attenuation of ring resonator

B. Dong, H. Cai, G. I. Ng, P. Kropelnicki, J. M. Tsai et al.

Citation: Appl. Phys. Lett. **103**, 181105 (2013); doi: 10.1063/1.4827096
View online: http://dx.doi.org/10.1063/1.4827096
View Table of Contents: http://apl.aip.org/resource/1/APPLAB/v103/i18
Published by the AIP Publishing LLC.

A nanoelectromechanical systems actuator driven and controlled by Q-factor attenuation of ring resonator

B. Dong,[1,2] H. Cai,[2] G. I. Ng,[1] P. Kropelnicki,[2] J. M. Tsai,[2] A. B. Randles,[2] M. Tang,[2] Y. D. Gu,[2] Z. G. Suo,[3,a)] and A. Q. Liu[1,b)]
[1]*School of Electrical and Electronic Engineering, Nanyang Technological University, Singapore 639798*
[2]*Institute of Microelectronics, A*STAR (Agency for Science, Technology and Research), Singapore 117685*
[3]*School of Engineering and Applied Sciences, Harvard University Cambridge, Massachusetts 02138, USA*

(Received 17 August 2013; accepted 7 October 2013; published online 29 October 2013)

In this Letter, an optical gradient force driven Nanoelectromechanical Systems (NEMS) actuator, which is controlled by the Q-factor attenuation of micro-ring resonator, is demonstrated. The actuator consists of a tunable actuation ring resonator, a sensing ring resonator, and a mechanical actuation arc. The actuation displacement can reach up to 14 nm with a measured resolution of 0.8 nm, when the Q-factor of the ring resonator is tuned from 15×10^3 to 6×10^3. The potential applications of the NEMS actuator include single molecule manipulation, nano-manipulation, and high sensitivity sensors. © *2013 AIP Publishing LLC*. [http://dx.doi.org/10.1063/1.4827096]

In the past decade, silicon based microelectromechanical systems (MEMS), especially MEMS actuators, are employed in a variety of optical, RF, and industrial applications, which offer on-chip integration with high reliability and low cost.[1,2] However, the micro-scale dimensions of MEMS actuators limit both the speed and precision of actuation. As the dimensions are scaled down to nano-scale, the traditional actuation methods, such as the electrostatic force, could be difficult to be realized because of the correspondingly decreased capacitance and increased impedance, making the devices susceptible to thermal noise and limiting their applications for high-resolution actuation.[3]

Nanoelectromechanical systems (NEMS) scale down the dimensions to nano-scale, which makes NEMS suitable for a multitude of technological applications such as ultrafast sensors, actuators, and signal processing components.[4] To realize effective NEMS actuators, optical gradient force has been one of attractive alternatives approaches due to its capability to generate mechanical deformation within nano-scale region.[5–9] Meanwhile, the optical gradient force can be increased in evanescently coupled nano-scale waveguides due to the enhanced gradient of the optical field intensity. The relationship between the actuation displacement and the input optical power has been discussed in previous work on opto-mechanical actuators.[3,10] To further enhance the optical gradient force, cavity enhancement, especially Whisper Gallery Mode (WGM) ring resonator, is employed to provide strong interaction for optical routing with low input energy due to its high Q-factor.[11–13] The high Q-factor ring resonator is capable to enhance the optical field intensity by orders of magnitude, which makes it possible to use optical gradient force for nano-scale actuation.

In this Letter, an active NEMS actuator driven by optical gradient force is demonstrated. The actuation displacement is controlled by tuning the Q-factor of the ring resonator through p-i-n electro-optics modulator, which induces free carriers into the resonator and changes its absorption coefficient. The mechanical actuator with nano-scale precision is optically driven by the enhanced optical gradient force, due to high Q-factor of ring resonators.

The NEMS actuator consists of a tunable actuation ring resonator, a sensing ring resonator, and a mechanical actuation arc. The two rings are optically linked through a bus waveguide, where light is coupled into and out of the two ring resonators as shown in Figure 1(a). Optical gradient force is generated between the actuation ring and mechanical arc nano-actuator while the actuation displacement is measured by the sensing ring. Part of the tunable ring resonator waveguide is rib waveguide, and the slab on each side is p- and n-type doped, respectively, forming a p-i-n junction. The schematic of the mechanical arc nano-actuator is shown in Figure 1(b), which is a 200-nm width doubly clamped silicon beam and the outer radius R is 20.3 μm. The central angle of central arc and side arcs are 30° and 15°, respectively. The mechanical arc is clamped by two anchors, so that it can move along the x direction but restrict the movement in the z and y directions. The outer radii of the actuation ring and sensing ring are 20 μm and 10 μm, respectively, which have the same width of 450 nm. The broadband light is coupled from the bus waveguide into the actuation ring, and then optical gradient force is conducted between the actuation ring and the mechanical arc nano-actuator, which pulls the nano-actuator towards the actuation ring. When increasing the current across the p-i-n junction, the Q-factor of the actuation ring is decreased, and the optical gradient force is reduced and the mechanical arc moves towards the sensing ring along x direction. The displacement Δg of the nano-actuator results in the change of effective refractive index Δn of the sensing ring, causing a red shift of sensing ring's resonance wavelength $\Delta\lambda_s$, as shown in Figure 1(c). Therefore, the displacement of the mechanical arc nano-actuator can be detected by the sensing ring through the induced wavelength shift.

The attractive optical gradient force in-between the actuation ring and mechanical arc nano-actuator is proportional to the optical power P_a inside the ring. When pumping a broadband light into the bus waveguide, light that meets

a)Electronic mail: suo@seas.harvard.edu
b)eaqliu@ntu.edu.sg

the resonance condition of the ring resonator accumulates inside the ring. Then, the optical power is enhanced due to the long photon life time inside the ring resonators. The photon life time can be measured by the Q-factor of ring resonators, which is the most pronounced parameter to monitor the light enhancement within ring resonators. Meanwhile, the Q-factor of the actuation ring is controlled by tuning the intrinsic absorption, which is realized by free carrier injection. The intrinsic absorption of the ring resonator waveguide is related with free carrier density, which is linearly related to the injection current. Meanwhile, owing to the weak dependence of silicon's refractive index on the electron-hold pair concentration, the refractive index change of the micro-ring has negligible effect on optical power attenuation. Therefore, by forward biasing the p-i-n junction, majority of the carriers are forced into the core, strongly affecting the absorption coefficient. The speed of the tunable ring modulator is in nano-second level and restricted by injection speed of electrons and holes.[14]

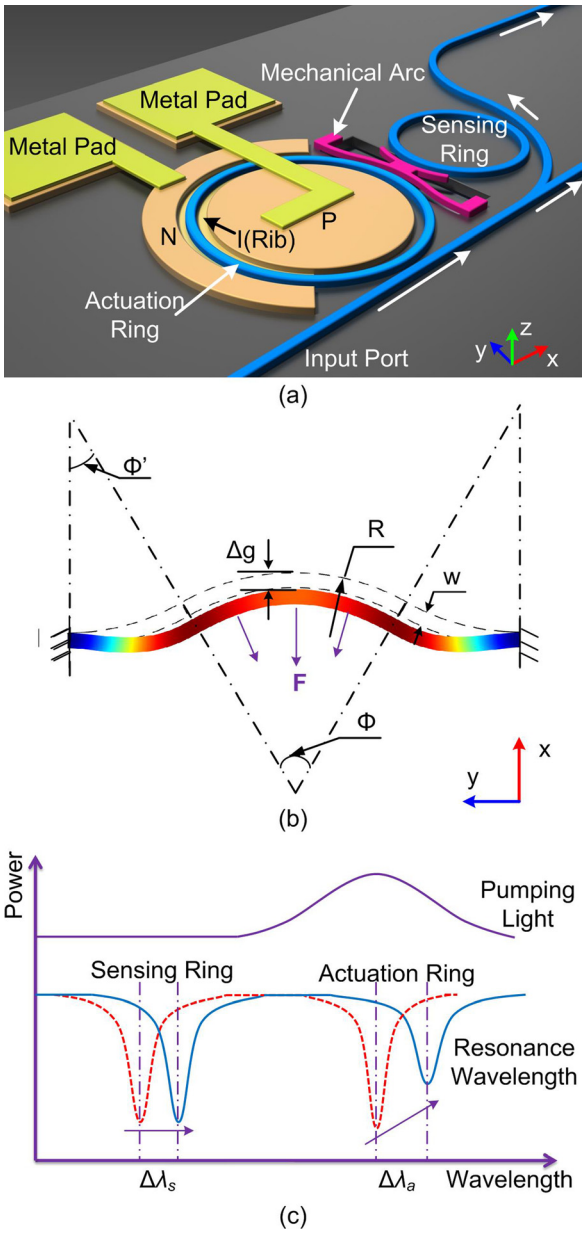

FIG. 1. (a) Schematic illustration of a nano-mechanical optical actuator driven by optical gradient force. (b) The mechanical design of the mechanical arc nano actuator and (c) working principle of the actuator, with schematic of the spectral response upon actuation.

The Q-factor is dominated by the external loss and the intrinsic loss, which are related with the coupling coefficient k and the absorption coefficient α, respectively. The Q-factor of ring resonator can be expressed as[11]

$$Q = \frac{\omega}{\Delta\omega_{FWHM}} = \frac{\pi n_{eff} L\sqrt{t\beta}}{\lambda(1-t\beta)}, \tag{1}$$

where ω is frequency of light, $\Delta\omega_{FWHM}$ is the full-wave half maximum at resonance, n_{eff} is the effective refractive index, L is effective perimeter of the actuation ring, t is the transmission coefficient of the waveguide-ring coupler, β is the single pass amplitude transmission, and λ is the resonance wavelength. The single pass amplitude transmission β is related with absorption coefficient α as $\beta^2 = e^{-\alpha L} = \beta_0^2 e^{-\Delta\alpha L}$, where β_0 is single pass amplitude transmission without injecting current. Therefore, when the coupling condition remains the same, the Q-factor is only related with the single pass amplitude transmission. By injecting more carriers, single pass amplitude transmission β decreases, and so does the Q-factor.

Due to Q-factor enhancement, the power within the ring resonator can be amplified $P_a = B \cdot P_{in}$, where B is the building-up factor and P_{in} is the optical power transmitting along the waveguide. The building-up factor B is defined as

$$B = \frac{k^2\beta^2}{(1-t\beta)^2}, \tag{2}$$

where t and k are the transmission coefficient and coupling coefficient between waveguide and ring, respectively. Both the building-up factor B and Q-factor are closely related with the round trip loss. By controlling the injection current across the p-i-n junction, β and α are modified. Therefore, B and Q can be controlled through the injection current, to realize direct control of the optical gradient force.

The deformation of the mechanical arc is due to the attractive optical gradient force. Without light, the gap between the mechanical arc and the sensing ring is g_0. The displacement of the mechanical arc Δg is related with normalized optical force as $F_{normalized} = K \cdot \Delta g$, where K is the effective spring constant of the silicon mechanical arc. We use Finite-difference time-domain (FDTD) software (COMSOL Multiphysics) to determine the displacement of the mechanical arc; the simulated displacement as a function of the optical power is shown in Figure 2. The inset in Figure 2 shows the deformation of the mechanical arc, while the red color indicates a larger deformation and the blue color indicates a smaller deformation. When the power inside the actuation ring is P_0, the force pulls the mechanical arc away from the sensing ring. Then, the gap in the middle becomes $g_0 + \Delta g$. The nano-scale displacement Δg is therefore related with the Q-factor, which can be expressed as

$$\Delta g = \frac{F}{K} = \left[-\frac{1}{\omega}\frac{d\omega}{dg}\bigg|_k \cdot \frac{L_{couple}}{v_g}\right] \cdot BP_{in} \cdot \frac{1}{K} = A \cdot Q^2, \tag{3}$$

where L_{couple} is the coupling length, v_g is the group velocity, and $A\left(=\left[-\frac{1}{\omega}\frac{d\omega}{dg}\Big|_k \cdot \frac{L_{couple}}{v_g}\right]\cdot\left[\frac{k^2\lambda^2}{(\pi n_{eff}L)^2 t}\cdot\beta P_{in}\right]\cdot\frac{1}{K}\right)$ is assessed coefficient factor. Therefore, Eq. (3) can be simplified as $\Delta g = A\cdot Q^2$. For a broadband light source, the Q-factor tuning coefficient A is considered to be constant due to multiple resonance wavelengths within spectrum range. The tuning efficiency $d(\Delta g)/dQ$, which is $A\cdot Q$, is increased for higher Q-factor. Therefore, the displacement Δg can be controlled by the Q-factor, which provides an effective control of the nanoelectromechanical actuator through varying the current of p-i-n junction between the ring resonators.

In addition, the nano-scale displacement of the mechanical arc is measured through the opto-mechanical effect. The normalized opto-mechanical coefficient g_{om} is defined as $g_{om} = \Delta n_{eff}/\Delta g$, which indicates the effective refractive index change (Δn_{eff}), when there is displacement of the mechanical arc. g_{om} can be treated as constant for small range displacement, so that the resonance wavelength shift is linearly related with the displacement as $\Delta\lambda \propto g_{om}\cdot\Delta g$. Therefore, the maximum displacement of the mechanical arc can be obtained by directly measuring the wavelength shift of the sensing ring, while the coefficient is derived from numerical simulation.

The NEMS actuator is fabricated by nano-photonic fabrication processes using standard silicon-on-insulator wafer, with a 220 nm thick silicon structure layer and a 2 μm buried oxide layer. Figure 3 shows the scanning electron microscope (SEM) image of a photonic NEMS actuator with two ring resonators and the mechanical arc. The waveguide structures have a width of 450 nm and a height of 220 nm for a single mode transmission. The mechanical arc is designed to have a width of 200 nm while the coupling gap between the actuation ring and the mechanical arc is 150 nm. The waveguides and ring resonators are patterned by deep UV lithography, followed by plasma dry etching to transfer the photo resist pattern into the structure layer. The rib structure of actuation ring has a 70-nm silicon slab layer for doping and metal via connection. The doping concentration for both p and n type are $2\times10^{14}\,\mathrm{cm}^{-3}$. After etching and doping, a 2-μm SiO_2 layer is deposited on the structure layers to ensure a low optical loss. A 40-nm Al_2O_3 is deposited and patterned, which is used as the protection film to protect those fixed structures and leave the window area for suspended structures open. Finally, HF vapor selectively undercut the buried oxide layer in the window area so as to release the parts of movable structures.

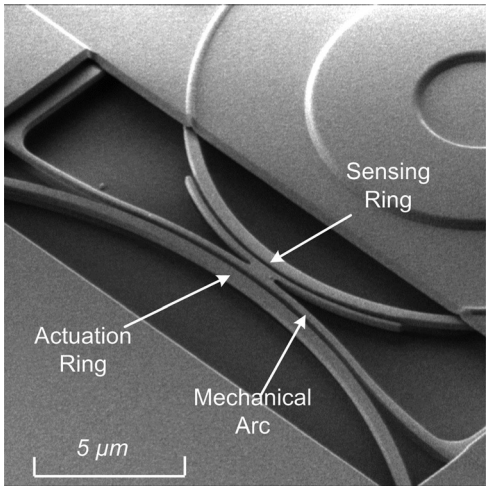

FIG. 3. SEM image of the NEMS actuator, which shows the mechanical arc nano-actuator with part of the actuating ring (left) and the sensing ring (right).

The experimental set-up for the nano-actuator characterization is shown in Figure 4. Light from a 12-dBm ASE light source (Amonics ALS-CL-13) is sent to a band pass filter (BPF) and amplified by Erbium Doped Fibre Amplifier (EDFA) (Amonics EDFA-CL-27). Due to the resonance wavelength shift of actuation ring, a 5-nm broadband pumping light is used to maintain a constant pumping light's power level, which is achieved through a combination of a broadband Amplified Spontaneous Emission (ASE) light source (>30 nm) and band pass filter. In order to obtain sufficient optical power for the actuation, an EDFA is employed for power amplification. The typical power level at the end of input tapered fiber is 20 mW. The amplified light is pumped into the silicon bus waveguide from tapered fiber through silicon waveguide mode converter. Then, the transmitted lights at both transmission ports are sent to an optical spectrum analyzer (OSA) (Ando AQ6317B) for analysis. Those lights with the wavelength match actuation ring's resonance wavelengths accumulate within the ring to generate the actuation optical force. After passing the actuation ring, the bus waveguide splits into two branches, so that 90% of the light is transmitted directly to the output port for analysis

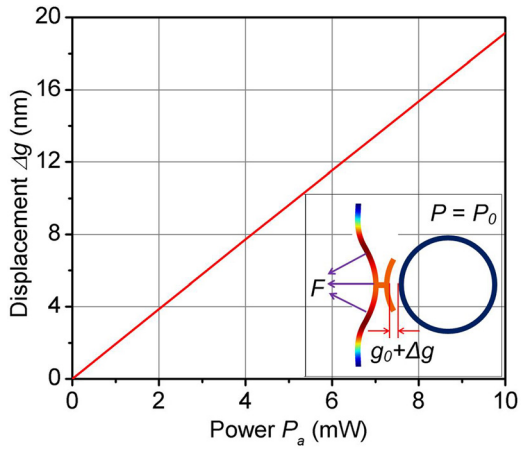

FIG. 2. The maximum displacement of the mechanical arc at various driving powers. The inset shows the simulated displacement of the mechanical arc.

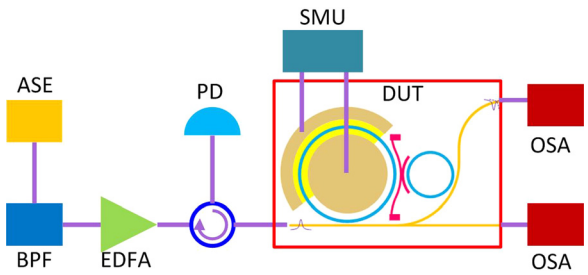

FIG. 4. Experimental setup of NEMS actuation measurement.

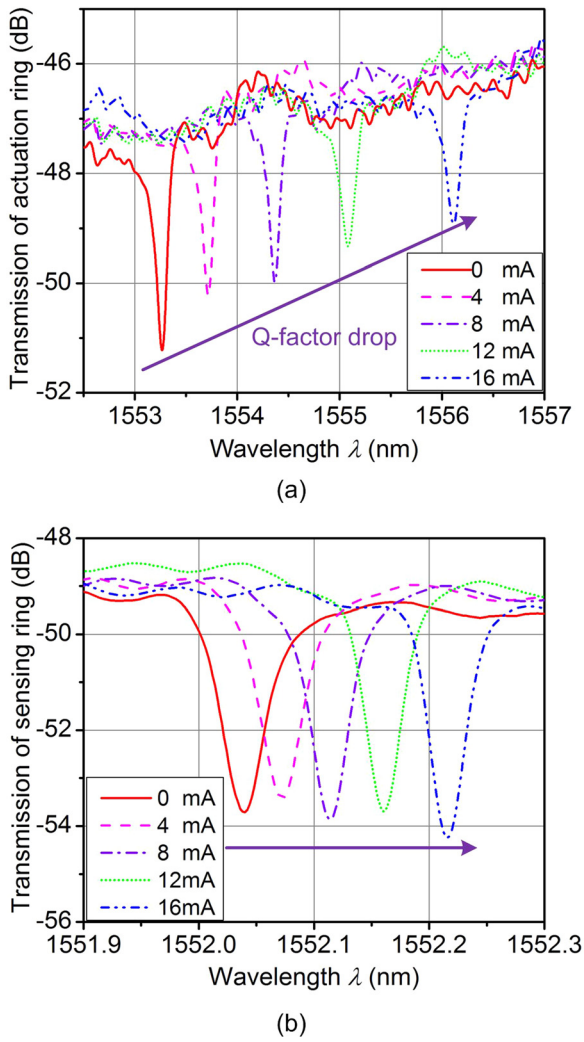

FIG. 5. Transmission spectrum of (a) actuation ring and (b) sensing ring when the tuning current across the p-i-n junction of the actuation ring resonator is increased from 0 to 16 mA.

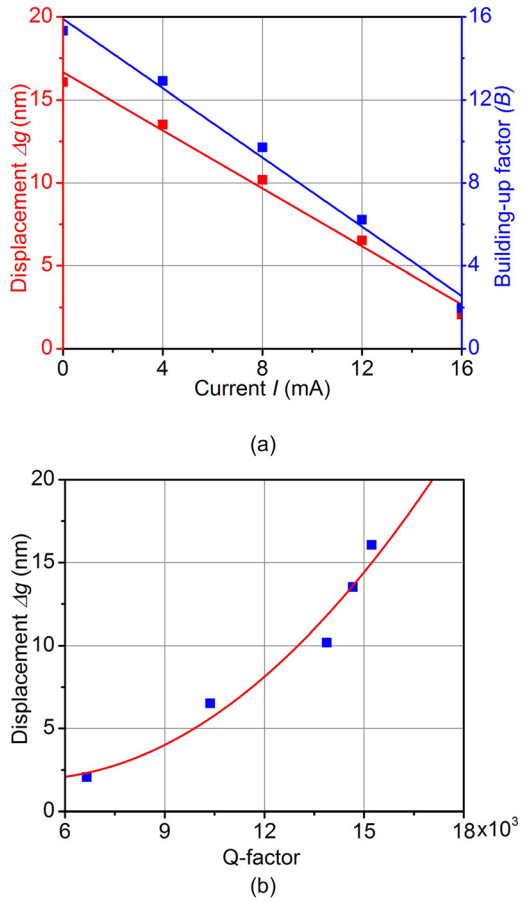

FIG. 6. (a) The maximum displacement of the mechanical arc and the building-up factor of actuation ring while increasing the driving current and (b) the displacement of the mechanical arc at variable Q-factor.

and only 10% of transmitted light is coupled to the sensing ring; thus, the optical gradient force between the sensing ring and the mechanical arc can be ignored. A source measurement unit (SMU) is connected with the metal pad to forward bias the p-i-n junction of the actuation ring for Q-factor tuning. By increasing the bias current, the transmission spectrum of both the actuation ring and sensing ring shift and are shown in Figure 5. During the experiments, the current is increased from 0 to 16 mA. By monitoring the spectrum of the actuating ring, the corresponding Q-factor of the actuation ring is decreased from above 15×10^3 to around 6×10^3 while the building-up factor B is decreased from 15 to only 1.7, as shown in Figure 6(a) and Table I. It shows that the drop in the Q-factor reduces the amplitude of circulating optical power and so does the optical gradient force. Thus, the mechanical arc nano-actuator move towards the sensing ring, causing the resonance wavelength of the sensing ring shifts 0.18 nm (from 1552.04 to 1552.22 nm), as shown in Figure 5(b). According to the calculation (through the opto-mechanical coefficient of sensing ring), such 0.18-nm wavelength shift corresponds to a 14 nm displacement of nano-actuator. The measured wavelength shift of the sensing ring based on OSA has a deviation approximately 5.5%. Due to linear relationship between wavelength shift and displacement, the accuracy of Δg is approximately 95%. The change of displacement Δg as function of building-up factor B and Q-factor are shown in Figures 6(a) and 6(b), which agrees well with the theoretical solution of the Eq. (3). Therefore, it indicates that the actuation can be achieved through the Q-factor tuning of the ring resonator. The sensitivity of the NEMS actuator is 0.875 nm/mA, while the resolution is 0.78 nm due to the detection limit of the optical spectrum analyzer (e.g., 0.01 nm).

In summary, a NEMS actuator based on Q-factor attenuation of the ring resonator is experimentally demonstrated. The optical actuator is driven by the evanescent wave coupled optical gradient force and controlled through Q-factor of actuation ring resonator. The nano-scale displacement is

TABLE I. Measured Q-factor of actuation ring and derived building-up factor B and displacement of mechanical arc nano-actuator Δg at different current levels.

Current (mA)	Sensing ring's wavelength (nm)	Q-factor	Building-up factor B	Displacement Δg (nm)
0	1552.040	15 226	15.32	16.059
4	1552.072	14 657	12.90	13.515
8	1552.114	13 878	9.71	10.176
12	1552.160	10 367	6.22	6.519
16	1552.216	6650	1.97	2.067

sensed through integrated sensing ring based on the opto-mechanical effects. A 0.18-nm wavelength shift is observed with 16 mA injected current, which corresponds to a driving distance of 14 nm. The proposed NEMS actuator has many merits such as small dimensions, low power consumption, and easy integration. These offer great potential for a wide span of nano-resonator based applications ranging from all-optical communications to fundamental sciences.

The authors would like to acknowledge the support from the Science and Engineering Research Council of A*STAR, Singapore, under SERC Grant No. 1021650084.

[1]X. M. Zhang, A. Q. Liu, D. Y. Tang, and C. Lu, Appl. Phys. Lett. **84**, 329 (2004).
[2]M. Malak, N. Pavy, F. Marty, Y. A. Peter, A. Q. Liu, and T. Bourouina, Appl. Phys. Lett. **98**, 211113 (2011).
[3]M. Ren, J. Huang, H. Cai, J. M. Tsai, J. Zhou, Z. Liu, Z. Suo, and A.-Q. Liu, ACS Nano **7**, 1676 (2013).
[4]H. G. Craighead, Science **290**, 1532 (2000).
[5]M. L. Povinelli, M. Loncar, M. Ibanescu, E. J. Smythe, S. G. Johnson, F. Capasso, and J. D. Joannopoulos, Opt. Lett. **30**, 3042 (2005).
[6]M. Li, W. H. P. Pernice, C. Xiong, T. Baehr-Jones, M. Hochberg, and H. X. Tang, Nature **456**, 480 (2008).
[7]J. F. Tao, J. Wu, H. Cai, Q. X. Zhang, J. M. Tsai, J. T. Lin, and A. Q. Liu, Appl. Phys. Lett. **100**, 113104 (2012).
[8]D. Van Thourhout and J. Roels, Nat. Photonics **4**, 211 (2010).
[9]G. S. Wiederhecker, L. Chen, A. Gondarenko, and M. Lipson, Nature **462**, 633 (2009).
[10]H. Cai, K. J. Xu, A. Q. Liu, Q. Fang, M. B. Yu, G. Q. Lo, and D. L. Kwong, Appl. Phys. Lett. **100**, 013108 (2012).
[11]W. Bogaerts, P. De Heyn, T. Van Vaerenbergh, K. De Vos, S. K. Selvaraja, T. Claes, P. Dumon, P. Bienstman, D. Van Thourhout, and R. Baets, Laser Photonics Rev. **6**, 47 (2012).
[12]H. Cai, B. Dong, J. F. Tao, L. Ding, J. M. Tsai, G. Q. Lo, A. Q. Liu, and D. L. Kwong, Appl. Phys. Lett. **102**, 023103 (2013).
[13]T. J. Kippenberg and K. J. Vahala, Science **321**, 1172 (2008).
[14]Q. Xu, B. Schmidt, S. Pradhan, and M. Lipson, Nature **435**, 325 (2005).